Turkish Journal of Engineering

Turkish Journal of Engineering (TUJE)
Vol. 3, Issue 1, pp. 25-31, January 2019
ISSN 2587-1366, Turkey
DOI: 10.31127/tuje.419531
Research Article

LASER CLADDING OF HOT WORK TOOL STEEL (H13) WITH TIC NANOPARTICLES

Tuncay Simsek [*1], Mahmut Izciler [2], Sadan Ozcan [3,4] and Adnan Akkurt [5]

[1] Mersin University, Architecture Faculty, Department of Industrial Design, Mersin, Turkey
tuncaysimsek@mersin.edu.tr
ORCID ID 0000-0002-4683-0152

[2] Gazi University, Technology Faculty, Department of Manufacturing Engineering, Ankara, Turkey
ORCID ID /0000-0002-0242-489X
mizciler@gazi.edu.tr

[3] Hacettepe University, Department of Physical Engineering, Ankara, Turkey
[4] Hacettepe University, Division of Nanotechnology and Nanomedicine, Ankara, Turkey
ORCID ID 0000-0001-7966-1845
sadan@hacettepe.edu.tr

[5] Gazi University, Industrial Design Engineering, Ankara, Turkey
ORCID ID 0000-0002-0622-1352
aakurt@gazi.edu.tr

* Corresponding Author
Received: 29/04/2018 Accepted: 06/08/2018

ABSTRACT
In this study, titanium carbide nanoparticles (TiC) were coated on the surface of X40CrMoV51 (H13) hot work tool steel by laser coating method. Two stage laser cladding method was employed for coating processes. In the first stage, TiC powders were mixed in the phonelic resin and precoated at 50 µm thickness on the surface of steel substrate under vacuum. In the second stage, laser was directed to the surface and then hard coating layers were obtained on the steel surfaces. A CO_2 laser with 2000 W power was operated at continuous-wave mode in the experiments. All laser cladding processes were performed under N_2 atmosphere and various laser powers were selected to show the effect of laser power on the quality of coated steel surfaces. The morphology and phase structures were examined by scanning electron microscopy, X-ray spectroscopy and optic microscope, respectively. The hardness of coating layers and bonding strength was defined with micro hardness tests and scratch test. The thickness of the coatings layers were measured in the range of 15-130 µm depending on laser powers. It is seen that crack-free, smooth and homogenous coating layers can be obtained at 237 W laser power. According to the hardness and micro-scratch tests results, hardness was improved significantly, and all coating layers had a good metallurgical strength to the substrate.

Keywords: *Laser Cladding, Nanoparticles, TiC, Tool Steel*

1. INTRODUCTION

With improvements in manufacturing technologies, the usage of tool steels has been increasing in recent years (Barra *et al*., 2003; Dosbaeva *et al*., 2015; Ozkul *et al*., 2017). Especially, H13 tool steel, which is widely used in plastic injection molding, casting, forging and extrusion etc., attracts significant attention due to its high elevated temperature strength, ductility, good annealing resistance and cost (Wei *et al*., 2011) Despite the fact that, H13 hot work tool steels are mostly used as structural material and intensively used in machine manufacturing, it is not preferred in the applications requiring high wear resistance due to its low wear properties. Particularly, under continuous mechanical and thermal loads, severe wears occur in tool steels (Medvedava *et al*., 2009; Luong *et al*., 1981) and these situations limits the usage of these materials (Bailey *et al.*, 2017; Telesang *et al.*, 2014; Mangour *et al.*, 2016). Therefore, in some cases to eliminate these problems whole part or relevant part of the workpieces are coated by various coating methods (Reza *et al.*, 2048; King *et al.*, 2004; Recco *et al.*, 2007). As it is known, while coatings improve the surface properties, it might also affect adversely the properties of the materials such as toughness, hardness etc. so that coating methods should be selected correctly according to substrate and coating materials. Recently, coating studies with nanoparticles showed that tribological and physical properties of materials can be improved significantly with usage of nanomaterials (Li *et al.*, 2006; Lehman *et al.*, 2012). Various methods are used for the coating of nanoparticles. Laser cladding method is one of the important method among them and it is intensively preferred in recent years. By using the superior features of laser beam, hard, homogenous, crackfree and nonporous layers with high wear and corrosion resistance can be obtained on the metal surfaces. A lot of coating studies with different laser sources can be seen in the literature. Most of these studies are conducted with CO_2 and Nd:YAG lasers but it is also seen that usage of fiber and diode laser are increased over time (Campanelli *et al.*, 2017; Yan *et al.*, 2017; Eerfanmanesh *et al.*, 2017; Weng *et al.*, 2017; Zhang *et al.*, 2017; Riverio *et al.*, 2014; Adraider *et al.*, 2012). All these studies specified that bonding between pre-cladding process and substrate before the cladding as well as selected laser parameters such as laser power, laser scanning speed, feed rate, diameter of laser spot, shielding gas and its pressure, play a fundamental role on quality of the cladding (Chew *et al.*, 2017; Cheng *et al.*, 2017; Weng *et al.*, 2017; Shi *et al.*, 2018; Emamian *et al.*, 2011).

In this study, TiC nanoparticles were pre-coated on the surface of H13 hot work tool steel under vacuum without any additive material and then laser clad at different laser powers by using 2 kW CO_2 laser while other parameters were kept constant. Coatings microstructures and bond strength to substrate were investigated.

2. EXPERIMENTAL METHOD

In laser cladding experiments, as coating material TiC nanoparticles with 10 nm crystallite size was used while commercial H13 tool steel was used as substrate. The steel substrate was prepared in the size of 100 (length) X 15 (width) X 1.5 (thickness) mm. The chemical composition of the substrate is given in Table 1 (Simsek, 2010).

Table 1. Chemical composition of DIN 1.2344 X40CrMoV51 (H13) tool steel

	C	Mn	Si	P	S	Cr	V	Mo	Fe
Chemical composition (Wt / %)	0.40	0.40	1.10	0.03	0.03	5.30	1.00	1.40	Bal.

Before the coating, the steel surfaces were sandblasted and cleaned with acetone-ethanol for purification from oil, rust and similar undesired contaminants. Phenolic resin was used in order to bond the nanoparticle to substrate. 5 wt% TiC nanoparticles were mixed with vinyl-phenolic resin (Araldit 71) and pre-coated at 50 µm thickness to metal surfaces carefully. In order to have a strong bond to metal surface, samples were dried in 20 mbar vacuum at 200 ˚C for 4 hours (Yilbas *et al.*, 2013). Prepared samples were exposed to the cladding process under N_2 atmosphere with 2 kW CO_2 laser (Amada, LC-2415 α III) at continuous-wave mode. Fig. 1 shows the schematic view of laser experiments setup.

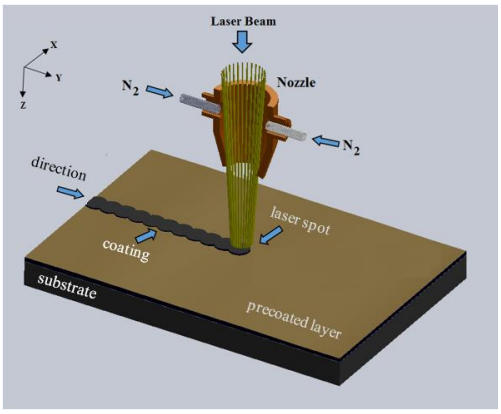

Fig. 1. The schematic view of laser experiments setups

Laser coating parameters are given in Table 2. The laser beam profile was Gaussian type. The laser beam focused on the layers was 300 µm in diameter and the nominal focal length of the lens was held at 127 µm. The overlapping ratio of the laser spot during the scanning was 80%, which formed continuous melting throughout the laser coating process. In the laser cladding experiments, laser energy density were changed while other parameters were kept constant. Table 2 shows the parameters selected during the cladding processes. These parameters were optimized after performing a series of experiments that provided the crack and cavity-free and non-porous coating layers. In the processing of materials, the following (Eq. 1) describes the energy density of a laser beam (also known as beam exposure). At sufficiently high energy densities, lasers can be used to cut through sheet metals, weld materials together, sinter powders together to form solids. Although, the energy density is an important indicator of energy input, there seems to be a strong correlation between energy density and some basic properties of laser coated parts such as porosity, microstructure and phase ratio at the surface

during coating.

$$E_\rho = P / (H.V) \quad (1)$$

where,
E_ρ = laser energy intensity ($J.cm^{-2}$) for single layer deposition
P = laser power (W)
H = Hatch space (μm) calculated as per [Overlap = (Spot size – Hatch space) / Spot size]
V = scan velocity ($cm.s^{-1}$)

Table 2. Laser cladding conditions

Average Laser Power	(W)	13, 73, 160, 237
Energy intensity	(J/cm^{-2})	$4.3x10^3$, $2.43x10^4$, $5.3x10^4$, $7.8x10^4$
Laser Wave Length	(μm)	10.64
Laser Beam Diameter	(mm)	0.3
Focal Length	(mm)	127
Frequency	(Hz)	1500
Scanning Speed	(cm/s)	0.5
Spot Diameter	(μm)	300
Hatch space (80% overlap)	(μm)	60
N_2 Pressure	(kPa)	200

Phase structures of nanoparticles were analysed by using X-Ray diffraction spectrophotometer (XRD, Rigaku, D/MAX-2200) with Cu–Kα radiation generated at 40 kV, 30 mA, in a range of 2θ from 20 to 80°, at 8°/min scanning rate. Scherrer's formula was used to calculate the crystallite size (Equation 2). In Equation 2, $\boldsymbol{\tau}$ represents the crystallite size, K is a constant taken depending on the crystal shape (0.89), λ is the x-ray wavelength (1.54Å), β is the full width at half maximum (FWHM) of the peak and θ is the Bragg angle. The FWHM and the position of (100) peak in the XRD pattern of TiC phase were used for crystallite size calculations. International Center for Diffraction Data (ICDD) powder diffraction files were used in the identification of crystalline phases.

$$\tau = \frac{K \,.\, \lambda}{B \,.\, Cos\,\theta} \quad (2)$$

Coated layers microstructures were characterized via optical microscope (Leica M205 C) and scanning electron microscope (FEI Quanta 200F). Laser coated specimens were cut by using a precise abrasive disc and polished by abrasives. For the microstructure examinations; the specimens were etched in a 5 % nital solution for 10 seconds. Micro hardness was measured by using a hardness tester (CSM instrument) under 200 mN load for 10 seconds with Berkovich B-K32 diamond tip. The measurements were repeated five times carefully in the similar area and the mean values were taken. The bond strengths were examined by scratch tester (CSM Instruments MST). In the scratch test; the load was applied in such a way that it would increase from 0.5 N to 20 N at 3 mm distance with a 100 μm diameter Rockwell diamond tool. Scratched surfaces were also examined by optical microscope (Simsek, 2010).

3. RESULTS AND DISCUSSION

The XRD pattern and SEM images of coating materials are given in Fig. 2. It is noticed that powders are consisted of cubic titanium carbide (ICDD Card No: 2-1179, cubic system, space group Fm-3m) (Sivkov et al., 2016). There were also some WC impurities because of worn of milling vial and balls used during synthesis procedures. It is seen that particles are mostly in irregular shape and morphology and crystallite sizes of the nanoparticles were calculated as approximately 10 nm by Scherrer's equation (Simsek, 2010).

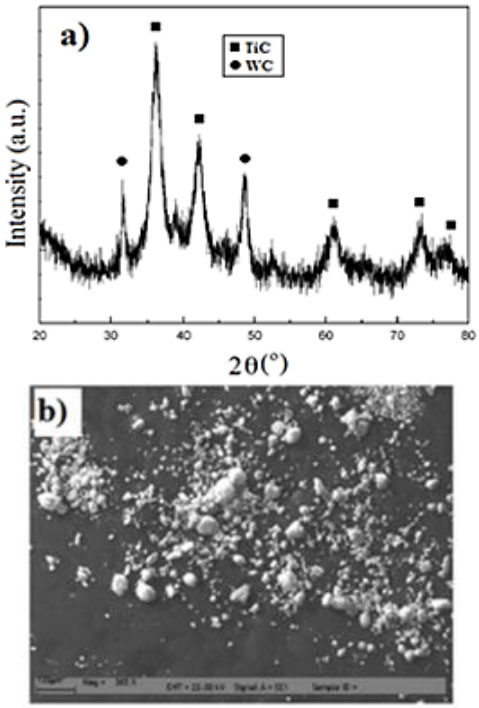

Fig. 2. a) XRD pattern and b) SEM images of the coating materials (Simsek, 2010).

Laser power was chosen in the range of 13-237 W in the experiments for the purpose of preventing any possibility of evaporation during the laser surface treatment. It seen that power below and above this values also caused the intensive crack and pores on the coated layers. The pictures of laser coating during process, precoated and laser treated surfaces are given in Fig. 3a-c, respectively.

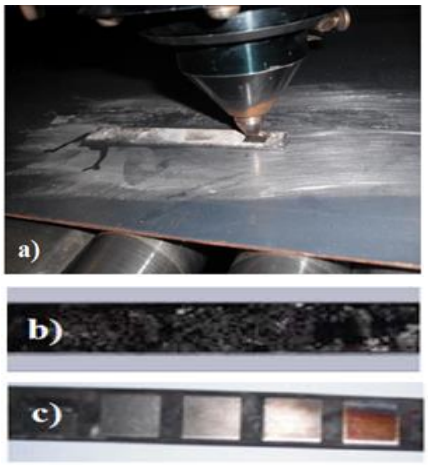

Fig. 3. a) Laser coating process b) Precoated samples c) Laser coated samples

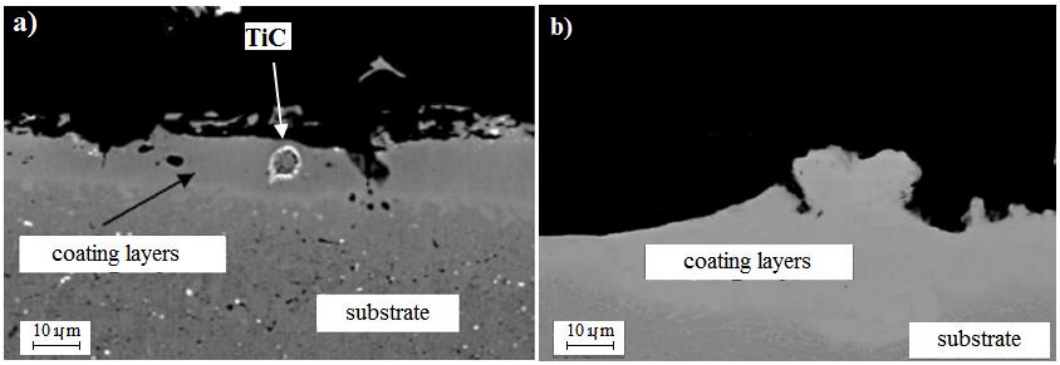

Fig. 4. SEM images of the laser coated layers a) 13 W laser power b) 73 W laser power

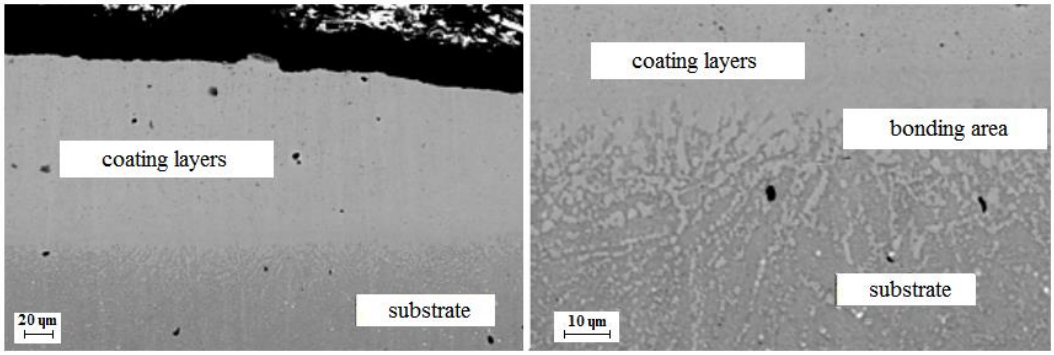

Fig. 5. SEM images of the laser coated layers at 237 W laser power

When the cross-section images in Fig. 4 were examined, it was seen that a thinner cladding layer was obtained at low laser power compared to high laser power (Fig. 5) since surface of base material was less molten. Cracks and cavities were observed on the surfaces of the samples cladded at 13-73 W laser power when compared to the cladding layers obtained at other high powers due to the thermal shocks caused by heat input and immediate cooling (Fig. 5). In the experiments with low laser power, there was no diffusion between the material surface and the coating material. It is also seen that the TiC nanoparticles were not dispersed homogeneously and agglomerated.

Thickness in the sample cladded at 13 W was determined as approximately 15 µm while thickness was not regular at the 73 W laser coated layers. At higher laser powers, transition amount of cladding material increased due to excess of melt amount occurring on the substrate surface. Thus, the thickness of the cladding layer was higher compared to the cladding layers obtained at lower powers (Fig. 5). Cracks and cavities occurring after rapid cooling decreased since there was a sufficient wetting between the ceramic phase and the substrate. It is also observed that the nearly similar problems were occurred with experiments conducted at 160 W laser power. However, no fractures and cavities were seen at layers obtained at 237 W laser power. This was attributed to the self-annealing effect of the layers formed by laser scanning tracks. Each scanned tracks modified the heat conduction and cooling rates in the coating area to be more thermally conductive. Furthermore, it was specified that cladding thickness was within the range of 110-130 µm depending on the increase in the laser power. Cross-sections examinations showed that coating layers with good metallurgical bond to the substrate can be obtained on the surfaces without any porosity and cracks (Fig. 5). Heat affected zone thickness was measured about 30 µm and gradually increased from cladding layer to the substrate. The results showed that the laser power was a very effective factor on the cladding quality (Simsek, 2010).

Comparative variation of the average hardness is given in Fig. 6. The measurements were repeated five times carefully in the similar areas and the mean values were taken into account. It was found that the hardness of substrate which was measured about 480 HV, increased up to approximately 1200 HV on the coated surface. In the experiments performed at low laser powers, the diffusion was very low and the substrate was melted less. Furthermore, due to the problems such as intensive cracks and pores, the hardness values were not taken properly so that the coated layers obtained at 237 W laser power were used in the microhardness and scratch tests. In literature, similar hardness values were also reported in Ignat *et al* studies. They specified that hardness of low carbon steel surface was increased from 200 HV to 1200 HV after cladding processes (Ignat *et al.*, 2003). In another study conducted by Jiang et al with TiC/H13 powder mixtures, they reported that after laser coating processes hardness of the AISI 4140 steel was increased from 200-250 HV to 860 HV (Jiang *et al.*, 2007).

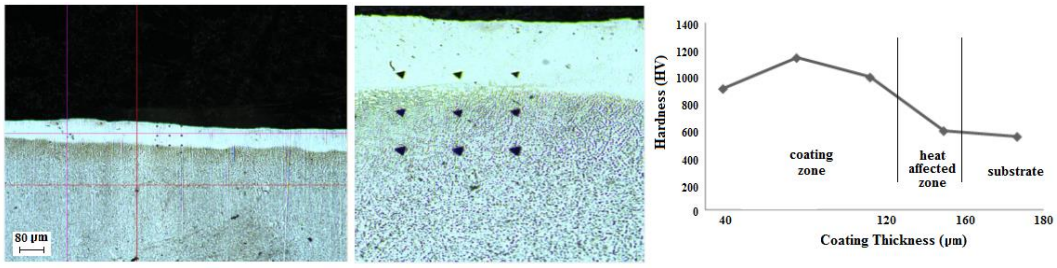

Fig. 6. Optic images and microhardness graphs of coated layers at 237 W (Simsek, 2010).

Normally, smooth surfaces are required for scratch tests otherwise the results can be deceived. Due to the nature of the laser coating process, the roughness of the surfaces after laser processing is not as smooth as the surfaces of the PVD or CVD coating. Scratch test results such as acoustic emission and penetration depth values, depending on the scratch distance were given in Fig. 7. Surface images of coated layers were also examined by optical microscope. It can be seen from acoustic emission graphs that critical load was 8.30 N at the 1.20 mm distance and scratch trace and surrounding small-sized fractures can be seen in the optic microscope images of the samples coated with 237 W laser power (Fig. 7a). Second critic load was observed around 12.20 N (Fig. 7b). Then continuous cracks were observed at 14.15 and continued up to 16.10 N load (Fig. 7c, d). Furthermore, it was seen that the penetration depth of the scratcher showed a regular increasing trend in the all coated layers.

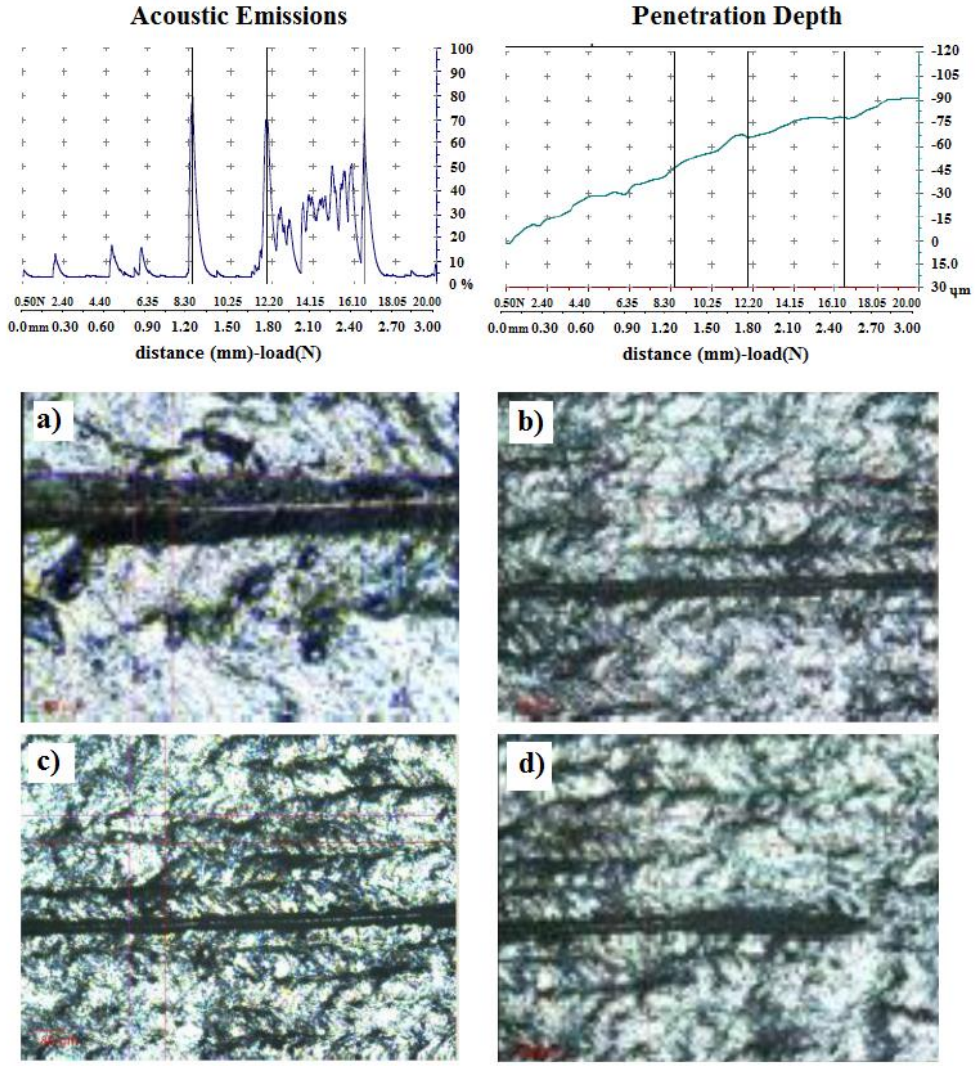

Fig. 7. Acoustic emission, penetration depth and optical microscope (X120) images of the coated layers under progressive load of 0.5-20 N

4. CONCLUSIONS

It is seen that TiC nanoparticles can be successfully coated to surface of H13 hot work tool steel under optimum conditions and careful precoating process. When the microstructures of the resulting coatings were examined, it is found that the laser power is very important factor on the coating quality. In the experiments with low laser power, there was no diffusion between the material surface and the coating materials. It is found that intensive cracks and pores were observed in the coatings and nanoparticles did not disperse homogeneously on the surfaces and get agglomerated. However, the most successful coatings were obtained at a thickness of approximately 130 μm at the surface of the H13 tool steel with the laser power of 237 W under N_2 atmosphere. The hardness was improved nearly 3 times when compared to substrate. It was also determined that hard and wear-resistant phases on the surface increased the resistance of the cladding layer against scratching.

REFERENCES

Adraider, Y., Hodgson S.N.B., Sharp, M.C., Zhang, Z.Y., Nabhani, F., Waidh, A. A., Pang, Y.X. (2012). "Structure characterisation and mechanical properties of crystalline alümina coatings on stainless steel fabricated via sol–gel technology and fibre laser processing." *Journal of the European Ceramic Society*, Vol. 32, pp. 4229–4240.

Bailey, N. S., Katinas, C., Shin Y. C. (2017). "Laser direct deposition of AISI H13 tool steel powder with numerical modeling of solid phase transformation, hardness, and residual stresses*." Journal of Materials Processing Tech,* Vol. 247, pp. 223–233.

Barrau, O., Boher, C., Gras, R., Rezai, A. F. (2003). "Analysis of the friction and wear behaviour of hot work tool steel for forging." *Wear*, Vol. 255, pp. 1444–54.

Campanelli, S. L., Angelastro, A., Signorile, C. G., Casalino, G. (2017). "Investigation on direct laser powder deposition of 18 Ni (300) marage steel using mathematical model and experimental Characterization." *International Journal of Advanced Manufacturing Technology*, Vol. 89, pp. 885–895.

Chew, Y., Pang, J. H., Bia, G, Song, B. (2017). "Effects of laser cladding on fatigue performance of AISI 4340 steel inthe as-clad and machine treated conditions." *Journal of Materials Processing Technology*, Vol. 243, pp. 246–257.

Cheng, Y.H., Cui, R., Wang, H.Z., Han, Z.T, (2017). "Effect of processing parameters of laser on microstructure and properties of cladding 42CrMo steel." *International Journal of Advanced Manufacturing Technology,* pp. 1-10.

Dosbaeva, G.K., El Hakim, M.A., Shalaby, M.A., Krzanowski, J.E., Veldhuis S.C. (2015). "Cutting temperature effect on PCBN and CVD coated carbide tools in hard turning of D2 tool steel." *International Journal of Refractory Metals and Hard Materials,* Vol. 50, pp. 1–8.

Emamian A., Corbin, S. F., Khajepour A. (2011). "The influence of combined laser parameters on in-situ formed TiC morphology during laser cladding." *Surface and Coatings Technology,* Vol. 206, pp. 124–131.

Erfanmanesh, M., Pour, H.A., Semnani, H.M., Razavi, R.S. (2017). "An empirical-statistical model for laser cladding of WC-12Co powder on AISI 321 stainless steel." *Optics and Laser Technology*, Vol. 97, pp. 180–186.

Ignat, S., Sallamand P., Nichici, A., Vannes, B., Grevey, D., Cicala, E. (2003). "$MoSi_2$ laser cladding—A new experimental procedure: double-sided injection of $MoSi_2$ and ZrO_2." *Surface and Coatings Technology*, Vol. 172, pp. 233–241.

Jiang, W.H., Kovacevic, R. (2007). "Laser deposited TiC/H13 tool steel composite coatings and their erosion resistance." *Journal of Materials Processing Technology*, Vol. 186, pp. 331–338.

King, P. C., Reynoldson, R. W., Brownrigg, A., Long, J. M. (2004). "Cr(N,C) diffusion coating formation on pre-nitrocarburised H13 tool steel." *Surface and Coatings Technology*, Vol. 179, pp. 18–26.

Lehman, E.B., Indyka, P., Bigos, A., Kot, M., Tarkowsk, L. (2012). "Electrodeposition of nanocrystalline Ni–W coatings strengthened by ultrafine alumina particles." *Surface and Coatings Technology,* Vol. 211, pp. 62–66.

Li, M., He, Y., Yuan, X., Zhang, S. (2006). "Microstructure of Al2O3 nanocrystalline/cobalt-based alloy composite coatings by laser deposition." *Materials and Design*, Vol. 27, pp. 1114–1119.

Luong, L.H.S., Heijkoop, T. (1981). "The influence of scale on friction in hot metal working." *Wear*, Vol. 71, pp.93–102.

Medvedeva A, Bergstrob, J., Gunnarssona, S., Anderssona, J. (2009). "High-temperature properties and microstructural stability of hot-work tool steels." *Mater Science and Engineering A*, Vol. 523, pp. 39–46.

Mangour, B.A., Grzesiak, D., Yang, J.M. (2016). "Nanocrystalline TiC-reinforced H13 steel matrix nanocomposites fabricated by selective laser melting." *Materials and Design,* Vol. 96, pp. 150–161.

Ozkul, I., Buldum, B.B., Akkurt A. (2017). "Regression Modeling of The Hole Qualities During Cold Work Tool Steels Drilling, With Different Characteristics Drill Bits." *Turkish Journal of Engineering,* Vol. 1, pp. 52-60.

Recco, A.C., Oliveira, I.C., Massi, M., Maciel, H.S., Tschiptschin, A.P. (2007). "Adhesion of reactive magnetron sputtered TINx and TICy coatings to AISI H13 tool steel." *Surface and Coatings Technology*, Vol. 202, pp. 1078–1083.

Reza, M. S., Aqida, S. N., Ismail, I. (2018). "Laser surface modification of Yttria Stabilized Zirconia (YSZ) thermal barrier coating on AISI H13 tool steel substrate."

IOP Conf. Series: Materials Science and Engineering, Vol. 319, pp. 1-4.

Riveiro, A., Mejías, A., Lusquiños, F. , Val J. D , Comesaña, R., Pardo, J., Pou, J. (2014). "Laser cladding of aluminium on AISI 304 stainless steel with high-power diode lasers." *Surface and Coatings Technology,* Vol. 253, pp. 214–220.

Shi Y, Li, Y, Liu, J., Yuan, Z. (2018). "Investigation on the parameter optimization and performance of laser cladding a gradient composite coating by a mixed powder of Co50 and Ni/WC on 20CrMnTi low carbon alloy steel." *Optics and Laser Technology,* Vol. 99, pp. 256–270.

Sivkov, A., Shanenkov, I., Pak, A., Gerasimov, D., Shanenkova, Y. (2016). "Deposition of a TiC/Ti coating with a strong substrate adhesion using a high-speed plasma jet." *Surface and Coatings Technology,* Vol. 291, pp. 1–6.

Şimşek, T. (2010). The laser coating of stainless steel and tool steel with nanotitanium carbide and investigation of the wear behaviour coating layers, Master Thesis, University of Gazi, Ankara, Turkey.

Telasang, G., Majumdar, J. D., Padmanabham, G., Tak, M., Manna, I. (2014). "Effect of laser parameters on microstructure and hardness of laser clad and tempered AISI H13 tool steel." *Surface & Coatings Technology,* Vol. 258, pp. 1108–1118.

Weng, F., Yu, H. , Chen, C. , Liu, J, Zhao, L , Dai, J., Zhao, Z. (2017). "Effect of process parameters on the microstructure evolution and wear property of the laser cladding coatings on Ti-6Al-4V alloy." *Journal of Alloys and Compounds,* Vol. 692, pp. 989-996.

Weng, F., Yu, H., Chen, C., Liu, J., Zhao, L., Dai, J., Zhao, Z. (2017). "Effect of process parameters on the microstructure evolution and wear property of the laser cladding coatings on Ti-6Al-4V alloy." *Journal of Alloys and Compounds,* Vol. 692, pp. 989-996.

Wei, M.X., Wang, S.Q., Wang, L., Cui, X.H., Chen, K.M. (2011). "Effect of tempering conditions on wear resistance in various wear mechanisms of H13 steel." *Tribology International*, Vol. 44, pp. 898–905.

Yan, H., Zhang P., Gao Q., Qin Y., Lic R. (2017). "Laser cladding Ni-based alloy/nano-Ni encapsulated h-BN self-lubricating composite coatings." *Surface and Coatings Technology*, 332, pp. 422–427.

Yilbas, B.S., Patel F., Karatas C. (2013). "Laser controlled melting of HSLA steel surface with presence of B4C particles." *Applied Surface Science*, Vol. 282, pp. 601– 606.

Zhang, P., Liu X., Yan H. (2017). "Phase composition, microstructure evolution and wear behavior of Ni-Mn-Si coatings on copper by laser cladding." *Surface and Coatings Technology,* Vol. 332, pp. 504–510.